Adaptive Methods of Two-Scale Edge Detection in Post-Enhancement Visual Pattern Processing

Zia-ur Rahman[†], Daniel J. Jobson[‡], Glenn A. Woodell[‡]
[†]Old Dominion University, Norfolk, VA 23529
[‡]NASA Langley Research Center, Hampton, Virginia 23681

ABSTRACT

Adaptive methods are defined and experimentally studied for a two-scale edge detection process that mimics human visual perception of edges and is inspired by the parvo-cellular (P) and magno-cellular (M) physiological subsystems of natural vision. This two-channel processing consists of a high spatial acuity/coarse contrast channel (P) and a coarse acuity/fine contrast (M) channel. We perform edge detection after a very strong non-linear image enhancement that uses smart Retinex image processing. Two conditions that arise from this enhancement demand adaptiveness in edge detection. These conditions are the presence of random noise further exacerbated by the enhancement process, and the equally random occurrence of dense textural visual information. We examine how to best deal with both phenomena with an automatic adaptive computation that treats both high noise and dense textures as too much information, and gracefully shifts from a small-scale to medium-scale edge pattern priorities. This shift is accomplished by using different edge-enhancement schemes that correspond with the (P) and (M) channels of the human visual system. We also examine the case of adapting to a third image condition, namely too little visual information, and automatically adjust edge detection sensitivities when sparse feature information is encountered. When this methodology is applied to a sequence of images of the same scene but with varying exposures and lighting conditions, this edge-detection process produces pattern constancy that is very useful for several imaging applications that rely on image classification in variable imaging conditions.

Keywords: Edge-detection, Adaptive Edge-detection.

1. INTRODUCTION

The subject of aviation safety has been in the news on quite a few occasions recently because of collisions and near-collisions between aircrafts either in mid-air or during the taxi and/or landing processes. While this problem occurs in all kinds of weather and illumination conditions, it tends to be aggravated when the weather conditions are poor since these inevitably lead to poor visibility conditions as well. With this as the background, we have been developing an external hazard detection scheme that combines edge-detection with smart image enhancement, a la the visual servo (VS).[1–3] The VS uses the multi-scale retinex (MSR) algorithm[4–6] to perform locally-adaptive, context-dependent, non-linear image enhancement that provides increased image contrast and brightness, and (relative) independence from illumination. The one drawback of this scheme is that it tends to enhance noise significantly as well. This can be a significant issue for imagery acquired under poor visibility conditions since the sensor signal-to-noise ratio (SNR) tends to be poor when the overall dynamic range of the scene is narrow and skewed towards the lower end of the range. However, information about the significant features in the image is contained fully in the edge features in the image. The edge representation also has the advantage that it is sparse and hence can lead to faster analysis, and it is relatively immune to noise since edges due to noise can be removed from the feature space. In this paper we develop and present modifications to a two-scale edge-detection scheme that was presented in a 2006 paper by Jobson et al.[7] In a companion paper in these proceedings, Woodell et al.[8] describe the impact of changing imaging conditions on the performance of correlating edge images.

Contact: Zia-ur Rahman (zrahman@odu.edu) is an Associate Professor at ODU. He is affiliated with the Electrical and Computer Engineering Department and the Virginia Modeling, Analysis and Simulation Center (VMASC). Daniel Jobson (daniel.j.jobson@nasa.gov) and Glenn Woodell (glenn.a.woodell@nasa.gov) are with the Electromagnetics and Sensors Branch at the NASA Langley Research Center.

2. BACKGROUND

In previous papers,[1,9] we showed that the visibility limit in a non-linear image enhancement environment was set by image sensor noise. This image enhancement process[4–6] was based upon the use of visual measures for contrast, lightness, and sharpness[9] in a smart VS feedback computation.[1] Experiments with the VS suggested the need to add additional controls to assess edge-detection performance in the presence of visually significant noise in the enhanced image. Noise is a visually significant factor only when the *feature* signal-to-noise ratio (FSNR) ≈ 1. The FSNR is distinct from the commonly used *root-mean-square* (RMS) SNR in that the FSNR is not measured globally over the whole image, but rather regionally across the feature under consideration. Given that the application of powerful non-linear enhancement algorithms produces a highly spatially-variable level of noise, sophisticated new methods are needed for edge-detection in the presence of severe noise. The level of noise can be viewed as two cases that are not necessarily distinct:

1. moderate levels of noise in darker and/or turbid regions of the original image can become visually significant in the enhanced image;
2. high noise levels in the original image may completely mask all visual information in the VS-processed image because of the strong locally-adaptive enhancements.

Figure 1 illustrates two enhanced images that represent these two stages of noise.

Figure 1. Illustration of non-linear image enhancement and impact of noise on visibility: (a) original image; (b) visual servo enhancement; (c) enhancement with moderate level of noise injected in original; (d) enhancement with very high level of noise injected in original.

In this paper we examine how to best deal with edge-detection in the presence of both these noise phenomena with an automatic adaptive computation that treats both high noise and dense textures as too much information, and gracefully shifts from small-scale to medium-scale edge pattern priorities. This shift is accomplished by using different edge-enhancement schemes that have at least some perceptual validity. Namely, we would like the detected edges for both noise and feature patterns to accord with the visual perception of these phenomena in real images. Noise that is not perceptible, and likewise, features that are not perceptible in the enhanced image should not be picked up by the edge detection procedure. Neurophysiological evidence suggests that visual perception has some built-in noise evasiveness. Visual perception is often described as a two-scale process, sometimes classified as the parvocellular (P) and magnocellular (M) subsystems. This is both an anatomical distinction[10] and a physiological distinction.[11, 12] In primate vision, the P-channel is associated with high acuity and coarse contrast sensitivity, while the M-channel is associated with coarse spatial resolution and high contrast sensitivity. This arrangement appears to eliminate all but large noise spikes from the P-channel, and provides some noise smoothing benefits due to spatial averaging in the M-channel. We also examine the case of adapting to a third image condition, namely too little visual information, and automatically adjust edge detection sensitivities when sparse feature information is encountered. When this methodology is applied to a sequence of images of the same scene but with varying exposures and lighting conditions, this edge-detection process produces pattern constancy that is very useful for several imaging applications that rely on image classification in variable imaging conditions.

3. EDGE DETECTION OF NOISE PATTERNS

In order to perform edge-detection in the presence of heavy noise and texture, we seek to develop a generic—and hence fully automatic—processing scheme which is aimed at producing a more abstract visual representation than can be achieved with static edge detection methods. This processing should perform gracefully in a perceptual sense in that the result should resemble what an etcher or cartoonist may render. A basic motivation for this is that we expect that the visual structural simplification which is accomplished will translate into improvements in higher level pattern recognition processing. Specifically, noise and dense texture are addressed in a unified fashion with identical processing applied to both. The goal of reducing the occurrence of the visually superfluous edge patterns is expected to benefit downstream pattern recognition by retaining only visually significant edge patterns while eliminating edge events that do not contribute to visual meaning, and, in fact, interfere with visual pattern recognition. The overall concept can then be thought of as a streamlining of the pattern information to enable a reduction in ambiguity in pattern recognition. Streamlining edge pattern data also contributes to computational efficiency by simply reducing the volume of data which is input into downstream pattern recognition processing. Figure 2 shows examples of the basic two-scale edge detection scheme. Our new method builds on this foundation and uses automatically varying threshold values and local analysis to eliminate dense edges that are more reminiscent of noise and/or texture.

The edge operator that we use is the commonly used Difference-of-Gaussian (DOG) convolution with zero-crossing edge detection. As an analog for the P- and M-channels, we use two scales of this operator and apply it to each color band. The P-channel analog is a smallest scale DOG convolution operator that takes the form,

$$\mathcal{P}[m_1, m_2] = 1 - c_1 e^{-(m_1^2+m_2^2)/\sigma_P^2} \quad (1)$$

$$\hat{\mathcal{P}}[\nu_1, \nu_2] = \delta[\nu_1, \nu_2] - c_1 e^{-\pi\sigma_P^2(\nu_1^2+\nu_2^2)} \quad (2)$$

where $[m_1, m_2]$ specifies the pixel location in Cartesian coordinates, $\sigma_P = 4$ pixels and

$$c_1 = \frac{M_1 M_2}{\sum_{m_1=0}^{M_1}\sum_{m_2=0}^{M_2} e^{-(m_1^2+m_2^2)/\sigma_P^2}}$$

ensures that $\sum_{m_1=0}^{M_1}\sum_{m_2=0}^{M_2}\mathcal{P}(m_1, m_2) = 0$. Equation 2 shows the Fourier transform of Equation 1: $\hat{\mathcal{P}}$ represents the Fourier transform version of $\mathcal{P}$ and $\delta[\nu_1, \nu_2] = 1$ if, and only if, $\nu_1 = \nu_2 = 0$ and is 0 otherwise. Either

Figure 2. Two examples of post-enhancement edge detection (combined P- and M-channel results) to illustrate approximate perceptual validity of edge detection process: (left) noisy image; (right) detected edge patterns.

the spatial or the spatial frequency form can be used in implementing the convolution. Equation 1 needs to be modified slightly to incorporate the point spread function (PSF) of the sensor optics* into the construction of the convolution operator. This function is shown in Figure 3 for $\sigma_P = 4$.

For the M-channel, the operator has about a 3 pixel center diameter, but the surround is much larger than three times the positive center diameter. This is somewhat larger than might be expected, but produces better results in diverse perceptual comparisons. The operator is given by:

$$\mathcal{M}[m_1, m_2] = e^{-(m_1^2+m_2^2)/\sigma_{M_1}^2} - c_2 e^{-(m_1^2+m_2^2)/\sigma_{M_2}^2} \quad (3)$$

$$\hat{\mathcal{M}}[\nu_1, \nu_2] = e^{-\pi\sigma_{M_1}^2(\nu_1^2+\nu_2^2)} - c_2 e^{-\pi\sigma_{M_2}^2(\nu_1^2+\nu_2^2)} \quad (4)$$

where $\sigma_{M_1} = 1.1$ pixels, $\sigma_{M_2} = 10$ pixels, and

$$c_2 = \frac{\sum_{m_1=0}^{M_1}\sum_{m_2=0}^{M_2} e^{-(m_1^2+m_2^2)/\sigma_{M_1}^2}}{\sum_{m_1=0}^{M_1}\sum_{m_2=0}^{M_2} e^{-(m_1^2+m_2^2)/\sigma_{M_2}^2}}$$

ensures that $\sum_{m_1=0}^{M_1}\sum_{m_2=0}^{M_2}\mathcal{M}[m_1, m_2] = 0$.

*This assumes that we can model sensor optics—a combination of the lens optical transfer function, and the aperture response of photodetector device—as a Gaussian.

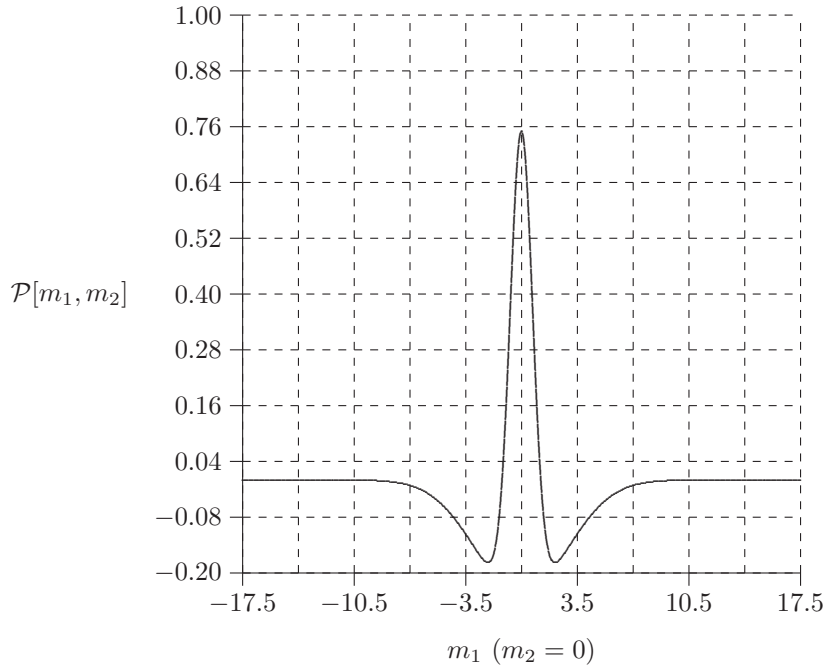

Figure 3: The P-channel convolution mask: $\sigma_P = 4, c_1 = 0.25$.

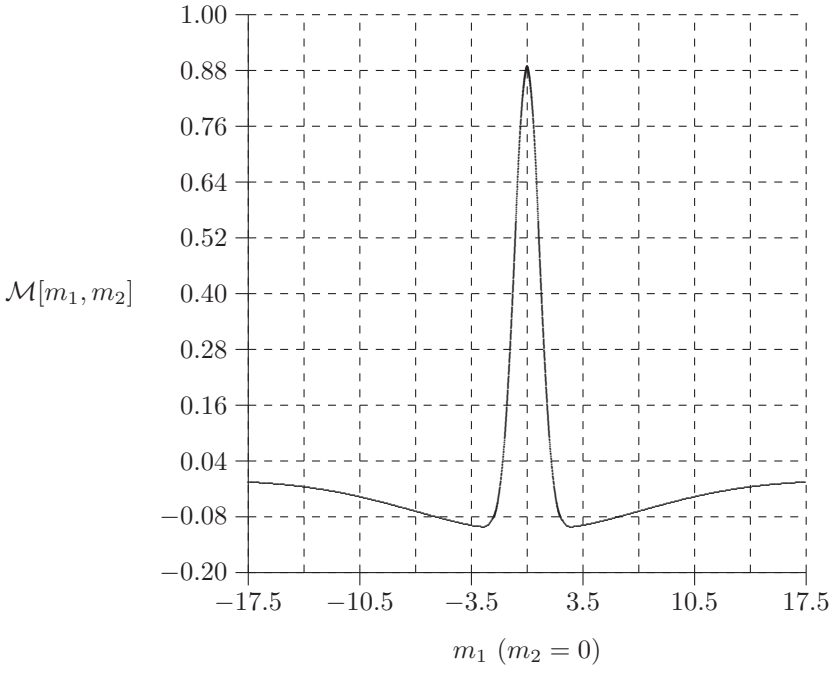

Figure 4: The M-channel convolution mask: $\sigma_{M_1} = 1.1$, $\sigma_{M_2} = 10$, $c_2 = 0.11$.

Within this system, a high threshold value for zero-crossing detection is employed in the P-channel—which responds only to very high contrast edges—and a much lower threshold is used in the M-channel—which provides a much higher contrast sensitivity, while providing noise avoidance through spatial averaging. Compared to the P-channel, the M-channel is about 3 times coarser in spatial resolution, but 5 times finer in contrast sensitivity. We do not attempt to incorporate in the edge-detection and analysis process, the temporal response differences between the P- and M-channels: the P-channel responds to sustained edge patterns, while the M-channel responds to transient edge phenomena. Several characteristics of noise show up as being distinct from visual feature information and these drive the task of detecting clean edges. Additionally, noise can be perceived as texture information, and vice versa, in many cases. In fact, some texture edge patterns, such as very fine weave textures at, or near, the spatial resolution limit, mimic noise rather convincingly. Some candidate distinctive characteristics that differentiate edges that arise from noise and those that arise from features are:

1. edge continuity or connectivity—features have it, noise does not;
2. edge spatial densities—noise has high, and regionally uniform densities, while features usually possess lower and much more variable densities. Even such dense feature data as printed text have word spaces and line spaces that prevent uniform high densities from persisting across significant regions of image space; and
3. edge orientations—features do not generally have random orientations, noise does.

The edge-detection scheme that we present in this paper uses just the second of these basic premises, and modifies the operation in two ways:

1. First, we add *adaptive* edge-detection thresholds for both the 1× scale associated with the P-channel, and the 3× scale associated with the M-channel.[†] The thresholds adapt to the number of edge-events, or computed edges, $\mathcal{E}_c$, in an image when compared to a pre-determined maximum allowable number of edges, $\mathcal{E}_m = 0.15 M_1 M_2$ for an $M_1 \times M_2$ image. If $\mathcal{E}_c > \mathcal{E}_m$, then the threshold is increased iteratively until either a threshold value is reached such that $\mathcal{E}_c < \mathcal{E}_m$, or, a maximum number of iterations has been performed. Increasing the threshold has the effect of reducing the number of edge-events that are actually classified as edges. Conversely, the threshold values are decreased iteratively if $\mathcal{E}_c < \mathcal{E}_m$. The criteria for $\mathcal{E}_m$ were established by large aggregate statistics for images with high signal-to-noise ratios. The major shortcoming of this approach is that when the edge-detection thresholds are adjusted adaptively—floated—, regionally high noise levels cause a loss of low contrast feature data which should clearly be retained.
2. Second, we considered that noise and dense texture needed to be treated as a *unified* phenomena in edge pattern-processing. In order for pattern-processing to converge on a concise visual representation, both noise and dense texture should cause a replacement of the 1× edge data by the 3× edge data which is essentially blurred feature data. This assumes that noise and texture both call for spatial averaging. Our premise is that noise is perceptually treated as a texture, so our processing should do so as well.

In order to develop this concept, we looked at the spatial characteristics of fine printed text because t produces the maximum perceptual pattern density for human observation. The major new idea here was that the characteristics of the printed text can be treated as having maximum edge density for both the 1× and 3× spatial scales, and that these characteristics can and should be applied at both the global and regional spatial scales of the image. Figure 5 hows an example of applying the 1× and 3× processing to a text image. The edge images are generated at twice the size of the original image in order to localize the edges with a half-pixel accuracy.[13–15] Experimental testing led to the development of a new scheme in which regional and global edge density criteria set by the spatial characteristics of printed text control the thresholds, τ_i and τ_{se} that are used to determine the edges. Additionally a new "self-erasure" process is also introduced. Self-erasure calls for

[†]The terms '1×' and '3×' are used to indicate that the P-channel uses a center that is one pixel wide, and the M-channel uses a center that is three pixels wide.

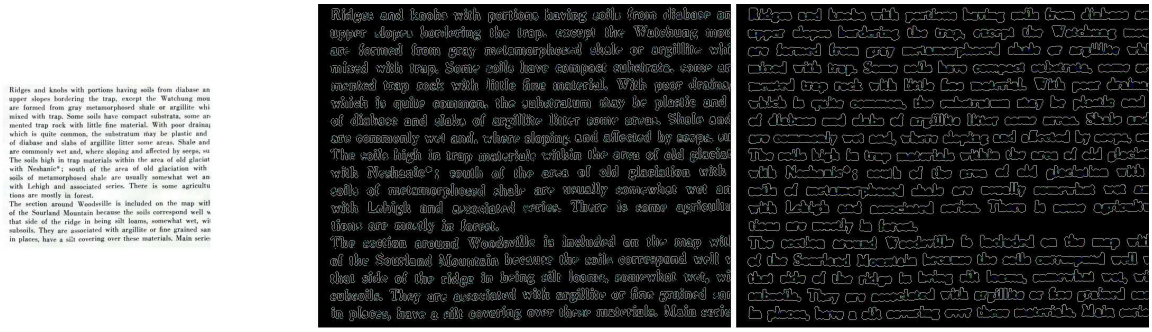

Figure 5. (left) Original image; (middle) 1× processing; (right) 3× processing: the edge images are generated at twice the resolution of the original images to localize edges with half-pixel accuracy.

erasing all edges in an $N_1 \times N_2$ region of the image—$N_1 < M_1, N_2 < M_2$—when the measured edge-density in that region exceeds a threshold τ_{se}. Both the global, adaptive threshold and regional self-erasure threshold eliminate noise and dense texture and act as an essential ingredient in achieving a perceptually graceful degree of visual abstraction for image regions that are either noisy or contain dense texture.

The edge adaptive scheme encompasses both noise evasion and dense texture handling using global properties of printed text. The edge-detection algorithm that we employ is made up of three distinct parts:

1. Two-scale edge-detection: the small scale P-channel which is high spatial resolution, high contrast, and the larger scale M-channel that has lower spatial resolution but picks low contrast edges. The P-channel operator uses adaptive "floating" thresholds to minimize the difference between the number of total edges found and the empirically determined optimal number of edges derived from dense text images. A fusion of the 3× and 1× data is used otherwise to produce the final two-scale edge output after going through steps 2 and 3 shown below.

2. Self-erasure: Each edge image is examined using regional 30×30 windows. If the number of regional edge pixels is found to be above the threshold τ_P for the 1× channel, and above τ_M for the 3× case, then the edge images are deemed to have noise- or dense texture-like properties, and all the edge pixels within those region are erased.

3. The final edge-fusion is performed by combining the self-erased data with the output of the 3× channel where the thresholds have been allowed to float until the number of computed edges is at or below the number of maximum allowable edge events. A modified self-erasure is used to perform the edge-fusion. The edge data from the self erased image is re-examined using 3×3 regional windows. If the number of edge-events in the regional window exceeds a threshold, then the data in that region is considered to have priority over the same region on the edge-data obtained from the output of the 3× channel. The data from the 3× channel is erased within the 3×3 block in such a case.

4. Variation on self-erasure is to skip steps 2 and 3, and combine the data using a slightly different rule. The edge image obtained from the 1× channel in step 1 is classified as noise if, after a maximum threshold has been exceeded, the total number of edge-pixels is still roughly twice as large as the maximum allowable number of edges. In this case, only the data from the 3× scale is used for edge-representation.

4. RESULTS

Since the self-erasure process tends to be very aggressive, care has to be taken to ensure that undesirable behavior is not evoked. We classify undesirable behavior as one of three conditions: (i) the 1× edge data is erased when it should have been retained to match perceived image structure; (ii) the 1× data that should have been erased is not erased, and this data suppresses the edge structures from the 3× channel that should

have won out; and (iii) unacceptable elimination of edge-structures in the final fused edge data. The scheme performs quite well overall, minimizing the occurrence of such behaviors. We note that there are a few special cases where these conditions are unavoidable. This suggests that filtering using print characteristics does not provide a complete solution to the issues that arise from noise/dense texture processing. Some examples where such problems can occur are:

1. small regions of fine print such as a sign set against a highly textured background like a hedge self-erase because the texture dominates the regional edge counts.
2. moderate noise levels that are insufficient to trigger 1× self-erasure when a better result would have been to replace the 1× pattern with 3× data.
3. high noise levels cause both 1× and 3× to self-erase completely. This can cause the final threshold for 3× processing to float too high and drop pattern structure that should have been retained. The visual result can then be a bit "too impressionistic".

Another more widespread trend in the testing is that more noise gets through than is desirable. This implies that a lot of visual noise is below the self-erasing criterion—i.e., below the density of printed text. This is clearly a performance limit due to the basic assumption of filtering by print spatial characteristics. Of course, a basic test goal was to be sure the processing passes all print from fine on up to larger fonts. The processing passes this test quite well with a very graceful transition from mostly 1× data dominating final result for fine print through a continuum of part 1× and 3× for transitional print fonts that are 2 pixels in feature width. Often these larger fonts are denser than fine print because line spaces are smaller. So for two-pixel wide fonts some 1× self-erasure occurs, but is filled in quite legibly by 3× data. Larger fonts that are high contrast shift back to the pattern data being mostly 1× data though this spatial resolution is not really required for legibility.

In Figure 6 we show an example in which we illustrate the output of the various steps involved in producing the final output in presence of severe noise. These steps include adaptive threshold processing, self-erasure and fusion. The final edge representation is a reasonable visual abstraction of the original enhance image. Figure 7 shows examples of an image with strong texture. The edge-processing successfully retains the texture patterns in the final rendition, even at the smallest scale. And, finally, Figure 8 shows a broad selection of results to establish generality and perceptual plausibility of the process.

The results shown in Figures 6, 7 and 8—and many other examples too numerous to show in this paper—support the assumption that printed text provides the densest spatial information that we need to pass through any edge filtering scheme. Additionally, noise and dense texture can, and should, be treated as a single pattern phenomena. On the whole the performance of the algorithm is perceptually graceful and plausible as a more abstract scene representation. The limitations, also apparent in the results, are that this assumption and the edge filtering based upon it work well only for dense textures, so this is not a full solution to texture processing. Coarse textures will be retained. Similarly the performance is reasonably good only for noise levels that generate sufficiently dense edge patterns to prompt self-erasure, and at really high levels of noise even the spatial averaging of 3× scale blurring is not enough to extract scene features from these really high noise level regions of an image. So noise speckle patterns remain for lower levels of noise, and noise patterns for very high noise are not removed by this processing.

5. CONCLUSION

We have presented a new algorithm for robust edge-detection in the presence of noise and dense texture. While adaptive thresholding has been used for edge-detection applications before, the key insight that this paper presents is that there is an optimal, or maximum acceptable, number of edges that can be determined by looking at the characteristics of fine text. This idea arises from the thought that the human eye-brain system experiences its greatest pattern recognition challenge when reading text of all sizes: it does seamless recognition at all text sizes and shapes. The other key idea that emerges from this paper is the concept of "self-erasure." Again, the idea emerges from the recognition that dense texture and noise share common characteristics. In

Figure 6. Example showing the performance of the edge-detection scheme on an image with severe degrees of noise: (top-left-top) original image; (top-left-bottom) MSR enhanced image; (top-middle) output of the 1× operator with adaptive thresholding; (top-right) output of the 3× operator with fixed threshold; (bottom-left) fused self-erased 1× and 3× outputs; (bottom-middle) output of the 3× operator with adaptive thresholding; (bottom-right) fusion of (bottom-left) and (bottom-middle).

fact, it can be hypothesized that noise and dense texture can, in fact, be treated as the phenomenon for visual processing. Self-erasure dictates that an optimal number of edges are acceptable within a local region of an image. If the number of edges exceeds this optimum, then the resultant image appears to be meaningless where the relational and contextual information between edges is lost, so it would be more useful to eliminate these edges altogether. We are also examining the scenario where, instead of completely eliminating these edges, we use a mechanism to reduce the number of regional edges to an acceptable level.

We have applied this edge-detection scheme to a variety of images, ranging from those encountered at consumer websites, to those that are of importance in detecting potential hazards on the runway during a landing approach. The common factor in the examples that we have shown is the presence of either dense texture or extreme noise. The algorithm produces encouraging results in eliminating spurious edges in these non-ideal subjects. The eventual goal of this approach is to use the generality of this approach to compare images of the same geographical area that are separated from each other in time. The separation in time results in changing image acquisition conditions such as amount and direction of illumination. If the impact of such conditions can be minimized then this can be used for comparing the images and detecting differences between them. This difference image can be used as an indicator of the presence of unwanted objects on a runway.

ACKNOWLEDGMENTS

The authors wish to thank the NASA Aviation Safety Program for the funding which made this work possible. In particular, Dr. Rahman's work was supported under NASA cooperative agreement NNL07AA02A.

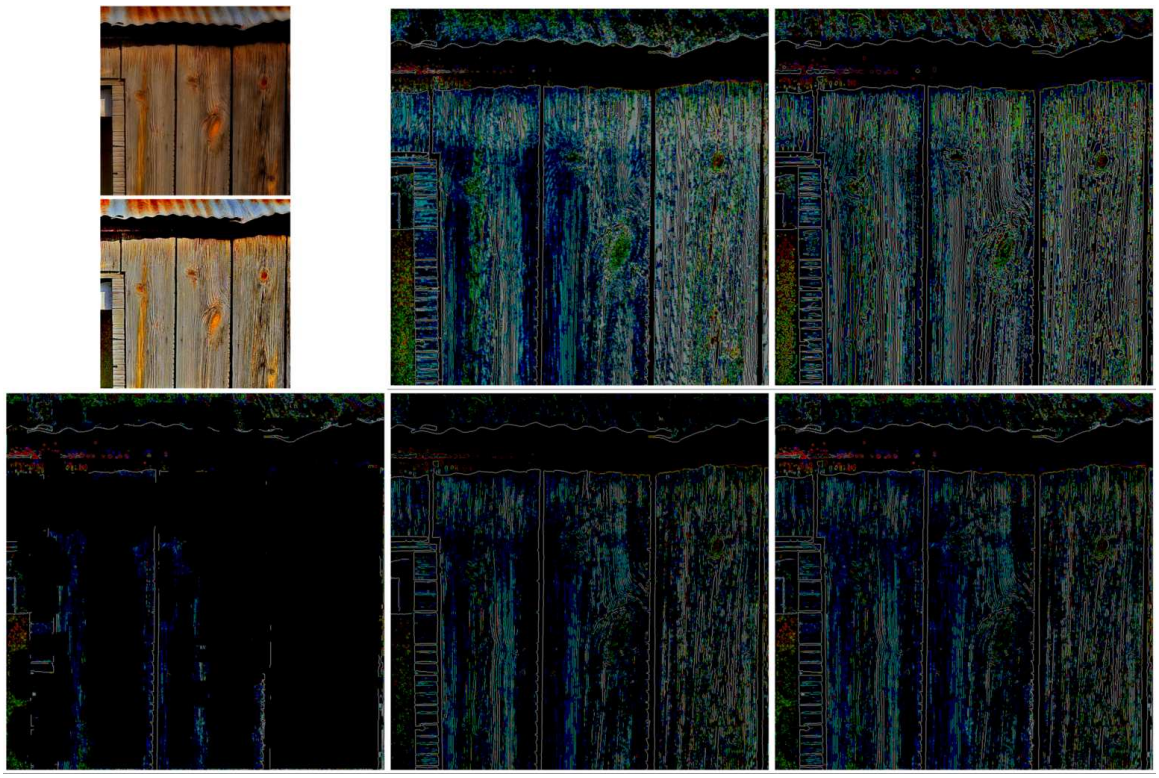

Figure 7. Example showing the performance of the edge-detection scheme on an image with strong degrees of texture: (top-left-top) original image; (top-left-bottom) MSR enhanced image; (top-middle) output of the 1× operator with adaptive thresholding; (top-right) output of the 3× operator with fixed threshold; (bottom-left) fused self-erased 1× and 3× outputs; (bottom-middle) output of the 3× operator with adaptive thresholding; (bottom-right) fusion of (bottom-left) and (bottom-middle).

REFERENCES

1. D. J. Jobson, Z. Rahman, and G. A. Woodell, "Feature visibility limit in the nonlinear enhancement of turbid images," in *Visual Information Processing XII*, Z. Rahman, R. A. Schowengerdt, and S. E. Reichenbach, eds., Proc. SPIE 5108, 2003.
2. D. J. Jobson, Z. Rahman, G. A. Woodell, and G. D. Hines, "The automatic assessment and reduction of noise using edge pattern analysis in nonlinear image enhancement," in *Visual Information Processing XIII*, Z. Rahman, R. A. Schowengerdt, and S. E. Reichenbach, eds., Proc. SPIE 5438, 2004.
3. G. A. Woodell, D. J. Jobson, Z. Rahman, and G. D. Hines, "Enhancement of imagery in poor visibility conditions," in *Sensors, and Command, Control, Communications, and Intelligence (C3I) Technologies for Homeland Security and Homeland Defense IV*, E. Carapezza, ed., Proc. SPIE 5778, 2005.
4. D. J. Jobson, Z. Rahman, and G. A. Woodell, "Properties and performance of a center/surround retinex," *IEEE Trans. on Image Processing* **6**, pp. 451–462, March 1997.
5. D. J. Jobson, Z. Rahman, and G. A. Woodell, "A multi-scale Retinex for bridging the gap between color images and the human observation of scenes," *IEEE Transactions on Image Processing: Special Issue on Color Processing* **6**, pp. 965–976, July 1997.
6. Z. Rahman, D. J. Jobson, and G. A. Woodell, "Retinex processing for automatic image enhancement," *Journal of Electronic Imaging* **13**(1), pp. 100–110, 2004.
7. D. J. Jobson, Z. Rahman, G. A. Woodell, and G. D. Hines, "A comparison of visual statistics for the image enhancement of foresite aerial images with those of major image classes," in *Visual Information Processing XV*, Z. Rahman, S. E. Reichenbach, and M. A. Neifeld, eds., Proc. SPIE 6246, 2006.

Figure 8: Examples showing the generality of the process: The layout is given as $\frac{\text{Originial}}{\text{Enhanced}}$ Edge-image.

8. G. A. Woodell, D. J. Jobson, and Z. Rahman, "Scene context dependency of pattern constancy of time series imagery," in *Visual Information Processing XVII*, Z. Rahman, R. A. Schowengerdt, and S. E. Reichenbach, eds., Proc. SPIE 6978, 2008.
9. D. J. Jobson, Z. Rahman, and G. A. Woodell, "The statistics of visual representation," in *Visual Information Processing XI*, Z. Rahman, R. A. Schowengerdt, and S. E. Reichenbach, eds., pp. 25–35, Proc. SPIE 4736, 2002. Invited paper.
10. Y. Shostak, Y. Ding, and V. A. Casagrande, "Neurochemical comparison of synaptic arrangements of parvocellular, magnocellular, and koniocellular geniculate pathways in owl monkey (*aotus trivirgatus*) visual cortex," *Journal of Comparative Neurology* **456**, pp. 12–28, 2003.
11. L. P. O'Keefe, J. B. Levitt, D. C. Kiper, R. M. Shapley, and J. A. Movshon, "Functional organization of owl monkey lateral geniculate nucleus and visual cortex," *Journal of Neurophysiology* **80**, pp. 594–609, August 1998.
12. N. H. Yabuta and E. M. Callaway, "Functional streams and local connections of layer4c neurons in primary visual cortex of the macaque monkey," *Journal of Neuroscience* **18**, pp. 9489–9499, November 1998.
13. D. J. Jobson, "Spatial vision processes: From the optical image to the symbolic structures of contour information," Tech. Rep. 2838, NASA, Washington, DC, November 1988. NASA Technical Paper.
14. D. J. Jobson, "Isolating contour information from arbitrary images," in *Visual Information Processing for Television and Telerobotics*, F. O. Huck, ed., pp. 177–190, NASA, 1989.
15. D. J. Jobson, "A discrepancy within primate spatial vision and its bearings on the definition of edge detection processed in machine vision," Tech. Rep. 102739, NASA, Washington, DC, September 1990. NASA Technical Memorandum.